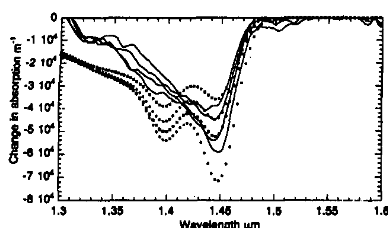

CFC4 Fig. 3 Comparison of absorption change between experimental data (lines) and numerical simulations (dots). The strength of absorption bleaching decreases with increasing bias.

ages incorporating a unit step function of 1 volt. The quantum-confined Stark effect was clearly evident for negative-applied voltages and absorption bleaching for positive voltages. Figure 3 shows a comparison between experimental data and the numerical simulations. Differences are attributed to doping uncertainty in the growth and the exciton broadening factor in the model. The broadening factor was set to 12 meV for both heavy and light holes. The heavy holes features are quite well matched but not the light holes. Filling the quantum well with electrons is not a sufficient condition to insure high-absorption changes.

In conclusion the InGaAsP system can provide comparable results to that of InGaAlAs. This opens the way to monolithically integrating the DBRAQWET structure with Al-free lasers sources and other components.

*Beckman Institut for Advanced Science and Technology, Departement of Electrical and Computer Engineering, University of Illinois, Urbana, Illinois 61801

1. M. Wegener, T. Y. Chang, I. Bar-Joseph, J. M. Kuo, D. S. Chemla, Appl. Phys. Lett. **55**, 583–585 (1989).
2. J. E. Zucker, T. Y. Chang, M. Wegener, N. J. Sauer, K. L. Jones, D. S. Chemla, IEEE Photon. Technol. Lett. **2**, 29–31 (1990).
3. N. Agrawal, D. Hoffmann, D. Franke, K. C. Li, U. Clemens, A. Witt, M. Wegener, Appl. Phys. Lett. **61**, 249–251 (1992).
4. M. Glick, R. Monnard, B. Dwir, J. F. Carlin, A. Rudra, M. A. Dupertuis, F. K. Reinhart, G. Weiser, Appl. Phys. Lett. **65**, 731–733 (1994).
5. J. Wang, J. P. Leburton, J. E. Zucker, IEEE J. Quantum Electron. **30**, 989–996 (1994).
6. J. F. Carlin, B. Dwir, M. Glick, R. Monnard, A. Rudra, M. A. Dupertuis, F. K. Reinhart, Mater. Sci. Eng. B **21**, 293 (1993).

CFC5 **9:00 am**

Vertical adjustment in surface-micromachined free-space micro-optical bench

L. Y. Lin, J. L. Shen, S. S. Lee, M. C. Wu, *UCLA, Electrical Engineering Department, 66-147D Engineering IV, Box 951594, Los Angeles, California 90095-1594*

Free-space micro-optical bench (FSMOB) fabricated by the surface-micromachining technique on Si substrate can integrate the entire free-space optical systems on a single chip.[1] Various out-of-plane free-space micro-optical elements such as three-dimensional microlens, mirror, and gratings have been demonstrated for FSMOB.[1,2] Micropositioners such as translation or rotation stages can also be fabricated by the same micromachining processes, which enables on-chip optical alignment or optical switching. Previously, we have demonstrated a self-aligned hybrid integration scheme for incorporating semiconductor lasers and other optoelectronic devices into the FSMOB.[3] Side-mounting scheme is employed to match the optical axes of the semiconductor laser and the micro-optical elements on Si FSMOB. In many other applications, the height of optical axis of the optoelectronic devices varies and cannot be directly matched. Vertical adjustment of the optical beams is necessary. However, most of the surface-micromachined actuators are designed for in-plane movement. Limited vertical translation (height direction) was demonstrated by the vertical comb array actuators.[4] In this paper, we report a novel adjustable optical beam-steering mirrors that can translate the in-plane movement of micro-optical elements into height adjustment of the optical beams. Adjustment of the optical axis height over 140 µm is successfully demonstrated.

The schematic diagram of the adjustable beam steering device is illustrated in Fig. 1(a). It consists of a pair of 45° mirrors, which changes the height of the optical beams without angular movement. The mirrors are fabricated by the microhinge technology. By integrating the upper mirror with a linear translation stage, then the in-plane movement of the mirror is effectively translated into the vertical adjustment of the optical axis. The scanning electron micrographs (SEM) of the beam steering device are shown in Figs. 1(b) and (c). The beam-steering mirrors are used to correct the optical axis of an upright-mounted semiconductor laser. The optical axis of the upright-mounted semiconductor laser is determined by the substrate thickness, which typically has a variation of more than 10 µm.

To characterize the performance of the beam-steering mirrors, a micro-Fresnel lens is also integrated to allow the measurement of far-field patterns. The vertical displacement of the imaged optical beams versus the in-plane translation of the upper mirrors is shown in Fig. 2. By moving the upper mirror by 140 µm, the height of the optical beam is varied by 140 µm. After passing the lens, a vertical displacement of 3.4 mm is observed. This is equivalent to a scanning angle of 5.5°. This type of vertical adjustment is very useful for micro-optical systems built on FSMOB. When combined with a comb drive actuator, it can be used to fine-adjust the vertical alignment of the optical beams. When combined with actuators

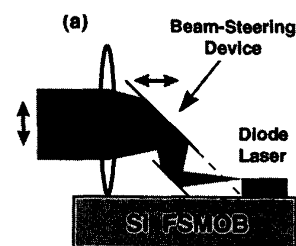

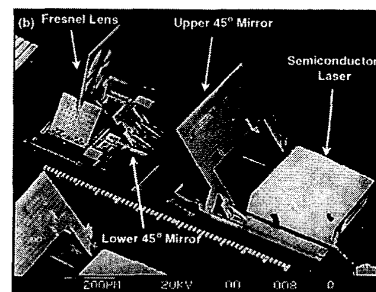

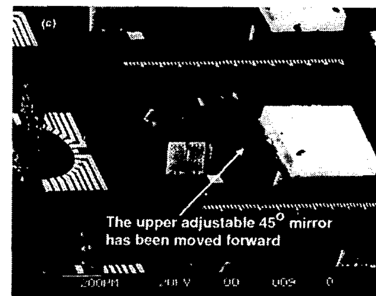

CFC5 Fig. 1 (a) The schematic drawing of the surface-micromachined beam-steering micromirrors. (b) and (c) The SEM micrograph of the 45° beam-steering mirrors integrated with a micro-Fresnel lens and a semiconductor laser.

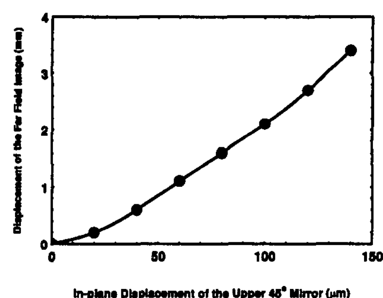

CFC5 Fig. 2 The vertical displacement of the far-field patterns versus the in-plane movement of the upper 45° mirror.

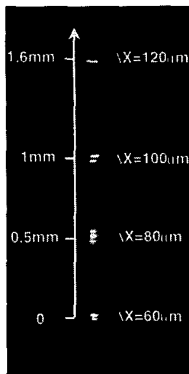

CFC5 Fig. 3 The CCD images of the scanned far-field patterns of the imaged beam from the integrated semiconductor laser for various positions of the upper 45° mirror.

with long travel distance, optical scanning or switching can be realized.

In summary, we have demonstrated a novel optical beam-steering device for vertical adjustment of the optical beams in the surface-micromachined free-space Si micro-optical bench. Vertical adjustment as large as 140 μm has been realized. When combined with an integrated microlens, a vertical scanning angle of 5.5° is also demonstrated.

1. L. Y. Lin, S. S. Lee, K. S. J. Pister, M. C. Wu, Photon. Technol. Lett. **6**, 1445 (1994).
2. O. Solgaard, M. Daneman, N. C. Tien, A. Friedberger, R. S. Muller, K. Lau, IEEE Photon. Technol. Lett. **7**, 41 (1995).
3. L. Y. Lin, S. S. Lee, K. S. J. Pister, M. C. Wu, Appl. Phys. Lett. **66**, 2946 (1995).
4. A. Selvakumar, K. Najafi, W. H. Juan, S. Pang, Proc. 1995 IEEE Micro Electro Mechanical Systems Workshop, Jan. 29–Feb. 2, 1995, Amsterdam, p. 43.

CFC6 **9:15 am**

Wafer-fused vertical-cavity bistable device at 1.55 μm wavelength

F. Jeannès, J. L. Oudar, R. Azoulay, A. Ougazzaden, *France Telecom, CNET-Paris B, BP 107, 92225 Bagneux Cedex, France*

All-optical switching devices can simplify optical networks by allowing optically controlled routing of signals, thereby avoiding the complexity of optical-to-electrical conversions. In this context vertical-cavity devices are very attractive, for their insensitivity to beam polarization and easy coupling to optical fibers. The realization of vertical-cavity structures at 1.55 μm suffers from the difficulty of growing high-reflectivity epitaxial mirrors lattice-matched to InP. In the context of vertical-cavity surface-emitting lasers, a new approach, based on wafer-fusion, has been very successful to overcome this difficulty.[1] In this technique, an InGaAsP/InP heterostructure, lattice-matched to InP is bonded to an AlAs/GaAs Bragg mirror, lattice-matched to GaAs. Here we present a vertical-cavity bistable device working at 1.55-μm wavelength, obtained by wafer fusion. It is an all-optical switching device, with no electrode, which uses the carrier-induced nonlinear refractive index of a bulk InGaAsP expitaxial layer.

The vertical-cavity structure was realized as follows. In a first stage, an InGaAsP/InP heterostructure and an AlAs/GaAs Bragg mirror were grown by metalorganic chemical vapor deposition on a (100) InP substrate and a (100) GaAs substrate respectively. On each wafer a sample of 5 × 5 mm² was cleaved. After cleaning, both samples were carefully deoxidised and immediately put in contact. Then they were uniformly pressed together within a graphite holder and loaded into a liquid-phase-epitaxy furnace. The furnace was heated up to a temperature of 630°C for 30 min in a purified H_2 flow. Then the InP substrate was removed using selective etching solutions. Finally an upper dielectric mirror was deposited. The cavity resonance had a width of 1 nm FWHM, corresponding to a finesse of about 130.

The nonlinear characteristics of these structures were studied in the reflection mode using a tunable laser source centered at 1.55 μm, with pulses of arbitrary temporal profile being generated by an acousto-optic modulator. In a free-space configuration, the beam was focused on the etalon at normal incidence through a ×10 microscope objective. We also investigated an optical fiber coupling configuration, where the optical fiber cleaved facet was put close to the top mirror of the device, the reflected beam being coupled back to the same fiber.

This device showed quite interesting characteristics. A switching threshold power of 0.7 mW was obtained, and a contrast ratio up to 60:1. In Fig. 1, bistable switching with a contrast ratio of 30:1 is displayed. Memory effect as long as several seconds was observed with manually adjusted incident intensities, though there was no active cooling of the device holder.

This bistable switching was obtained by tuning the laser wavelength onto the short wavelength side of the cavity resonance and was due to the carrier-induced dispersive nonlinearity. We measured the nonlinear index variations of the InGaAsP layer using the technique described by Sfez *et al.*[2] As shown in Fig. 2(a), the wavelength of the reflectivity peak shifts and becomes asymetric with increasing incident power. From these wavelength shifts, the nonlinear index change vs intracavity intensity was deduced [Fig. 2(b)]. Some saturation of the nonlinear index change was observed. The saturating value of the nonlinear index change was measured to be $\delta n_s = 3.1 \times 10^{-2}$ at a wavelength corresponding to a linear absorption coefficient of 100 cm^{-1}. The intracavity intensity needed to reach $\delta n_s/2$ is I_s = 54 kW/cm², corresponding to a calculated value for $n_2 = \delta n_s/I_s$ of about 0.6×10^{-6} cm²/W.

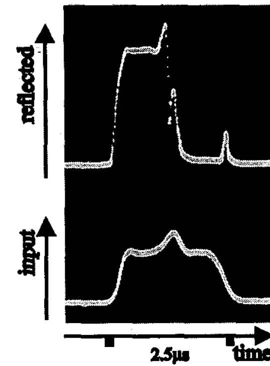

CFC6 Fig. 1 Input and output pulses showing the bistable memory effect, with a switching contrast of 30:1. The input plateau is 0.9 mW.

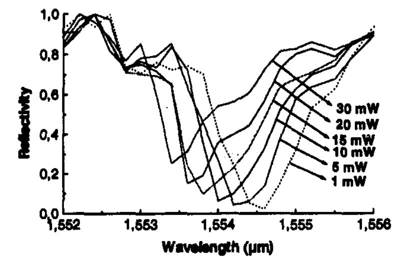

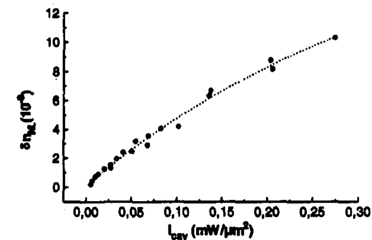

CFC6 Fig. 2 (a) Experimental reflectivity curves at various incident powers. (b) Nonlinear index change vs intracavity intensity, deduced from the reflectivity curves.

In conclusion we have demonstrated a new all-optical device operating at 1.55-μm wavelength, with submilliwatt threshold and large contrast ratio. It was realized by wafer fusion of an InGaAsP/InP active heterostructure onto a AlAs/GaAs Bragg mirror. Finally the carrier-induced dispersive nonlinearity of the InGaAsP active layer has been investigated.

1. D. I. Babic, J. J. Dudley, K. Streubel, R. P. Mirin, J. E. Bowers, E. L. Hu, Appl. Phys. Lett. **66**, 1030 (1995).
2. B. Sfez, R. Kuszelewicz, J. L. Oudar, Opt. Lett. **16**, 855 (1991).